CHAPTER 7

SCINTILLATION COUNTING

Radiation of various types is widely utilized for non-destructive inspection and testing such as in medical diagnosis, industrial inspection, material analysis and other diverse fields. In such applications, radiation detectors play an important role. There are various methods for detecting radiation.[1][2][3][4] *For example, typical detectors include proportional counters, semiconductor detectors that make use of gas and solid ionization respectively, radiation-sensitive films, cloud chambers, and scintillation counters.*

In scintillation counting, the combination of a scintillator and photomultiplier tube is one of the most commonly used detectors for practical applications.[5][6] *Scintillation counting has many advantages over other detection methods, for example, a wide choice of scintillator materials, fast time response, high detection efficiency, and a large detection area. This section gives definitions of photomultiplier tube characteristics required for scintillation counting and explains their measurement methods and typical data.*

7.1 Scintillators and Photomultiplier Tubes

When ionizing radiation enters a scintillator, it produces a fluorescent flash with a short decay time. This is known as scintillation. In the case of gamma rays, this scintillation occurs as a result of excitation of the bound electrons by means of free electrons inside the scintillator. These free electrons are generated by the following three mutual interactions: the photoelectric effect, Compton effect, and pair production. The probability of occurrence of these interactions depends on the type of scintillators and the energy level of the gamma rays. Figure 7-1 shows the extent of these interactions when gamma-ray energy is absorbed by a NaI(Tl) scintillator.

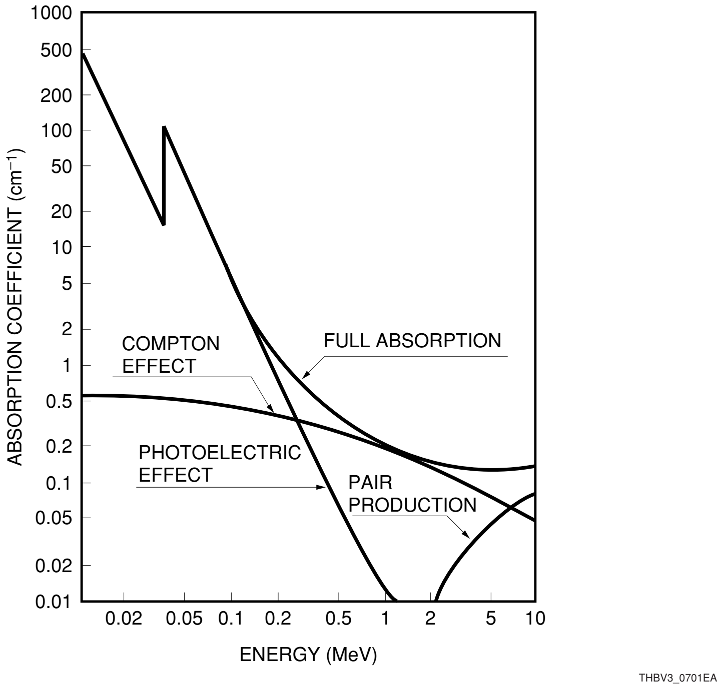

Figure 7-1: Gamma-ray absorption characteristics of NaI(Tl) scintillator

From Figure 7-1, it is clear that the photoelectric effect predominates at low energy levels of gamma rays, but pair production increases at high energy levels. Of these three interactions, the amount of scintillation produced by the photoelectric effect is proportional to gamma-ray energy because all the energy of the gamma ray is given to the orbital electrons. The photomultiplier tube outputs an electrical charge in proportion to the amount of this scintillation, as a result, the output pulse height from the photomultiplier tube is essentially proportional to the incident radiation energy. Accordingly, a scintillation counter consisting of a scintillator and a photomultiplier tube provides accurate radiation energy distribution and its dose rate by measuring the photomultiplier tube output pulse height and count rate. To carry out energy analysis, the current output from the photomultiplier tube is converted into a voltage output by an integrating preamplifier and fed to a PHA (pulse height analyzer) for analyzing the pulse height.[2] A typical block diagram for scintillation counting is shown in Figure 7-2.

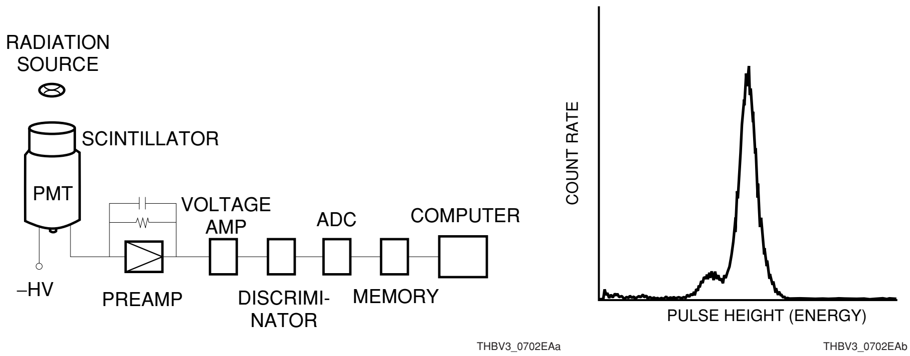

Figure 7-2: Block diagram for scintillation counting and pulse height distribution

Scintillators are divided into inorganic scintillators and organic scintillators. Most inorganic scintillators are made of a halogen compound such as NaI(Tl), BGO, BaF_2, CsI(Tl) and ZnS. Of these, the NaI(Tl) scintillator is most commonly used. These inorganic scintillators offer advantages of excellent energy conversion efficiency, high absorption efficiency and a good probability for the photoelectric effect compared to organic scintillators. Unfortunately, however, they are not easy to handle because of deliquescence and vulnerability to shock and impact. Recently, as an alternative for NaI(Tl) scinitillators, YAP:Ce with high density and no deliquescence has been developed. Other scinitillators such as LSO:Ce and GSO:Ce have also been developed for PET (Positron Emission Tomography) scanners.

Organic scintillators include plastic scintillators, liquid scintillators and anthracene of organic crystal. These scintillators display a short decay time and have no deliquescence. Plastic scintillators are easy to cut and shape, so they are available in various shapes including large sizes and special configurations. They are also easy to handle. In the detection of gamma rays, organic scintillators have a low absorption coefficient and exhibit less probability for the photoelectric effect, making them unsuitable for energy analysis applications. Table 7-1 shows typical characteristics and applications of major scintillators which have been developed up to the present.

Scinti-llators	Density (g/cm^3)	Emission Intensity (NaI(Tl) normalized at 100)	Emission Time (ns)	Peak Emission Wavelength (nm)	Applications
NaI(Tl)	3.67	100	230	410	Surveymeter, area monitor, gamma camera
BGO	7.13	15	300	480	PET
CsI(Tl)	4.51	45 to 50	1000	530	Surveymeter, area monitor
Pure CsI	4.51	<10	10	310	High energy physics
BaF2	4.88	20	0.9/630	220/325	TOF, PET, high energy physics
GSO:Ce	6.71	20	30	310/430	Area monitor, PET
Plastic	1.03	25	2	400	Area monitor, neutron detection
LSO:Ce	7.35	70	40	420	PET
PWO	8.28	0.7	15	470	High energy physics
YAP:Ce	5.55	40	30	380	Surveymeter, compact gamma camera

Table 7-1: Typical characteristics and applications of scintillators

A scintillator is attached to a photomultiplier tube with coupling material as shown in Figure 7-3. The coupling material is used in place of an air layer in order to minimize optical loss between the scintillator and the photocathode faceplate. Silicone oil having an index of refraction close to that of the glass faceplate is most widely used as a coupling material. However, selecting the proper material which provides good transmittance over the emission spectrum of the scintillator is necessary. Figure 7-4 indicates typical emission spectra of major scintillators and photocathode spectral responses of photomultiplier tubes.

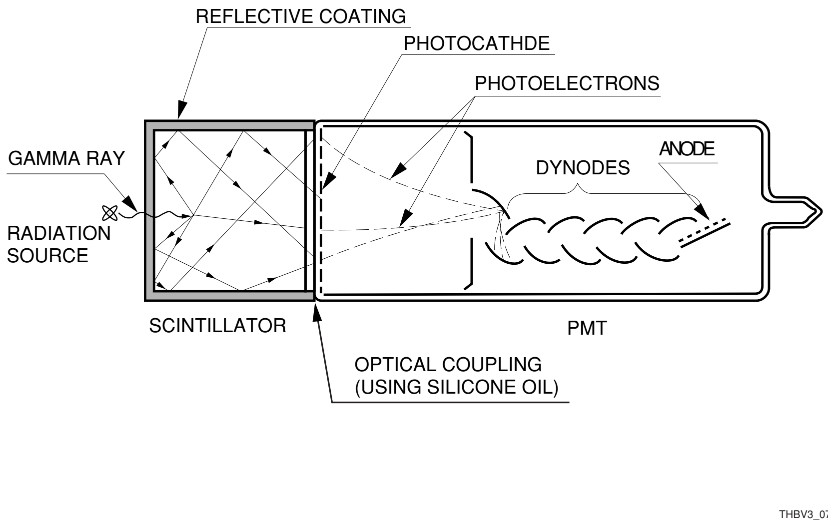

Figure 7-3: Gamma-ray detection using a NaI(Tl) scintillator and a photomultiplier tube

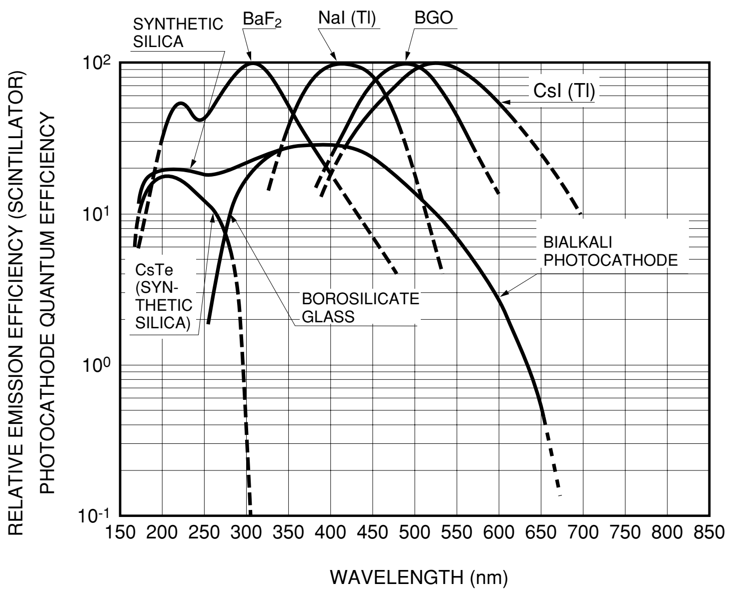

Figure 7-4: Photocathode quantum efficiency and emission spectra of major scintillators

7.2 Characteristics

(1) Energy resolution

There are two measurement methods in scintillation counting. One is the spectrum method that use a pulse height analyzer to measure an energy spectrum. The other is the counting method (described later on) that does not use a pulse height analyzer. In the spectrum method, pulse height discrimination is very important to determine photoelectric peaks produced by various types of radiation. This is evaluated as "energy resolution" or "pulse height resolution (PHR)".

Energy resolution is defined by the following equation using Figure 7-5. It is generally expressed as a percent:

$$R = \frac{\Delta P}{P} \qquad \text{(Eq. 7-1)}$$

R : energy resolution
P : peak value
ΔP : FWHM (Full width at half maximum)

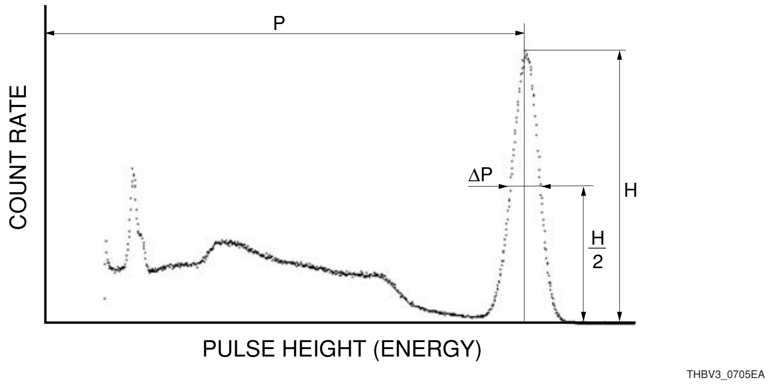

Figure 7-5: Definition of energy resolution

Figure 7-6 shows typical pulse height distributions for characteristic X-rays of ^{55}Fe and various kinds of gamma rays (^{57}Co, ^{137}Cs, ^{60}Co) detected by a photomultiplier tube coupled to an NaI(Tl) scintillator (measured using the same method as in Figure 7-2).

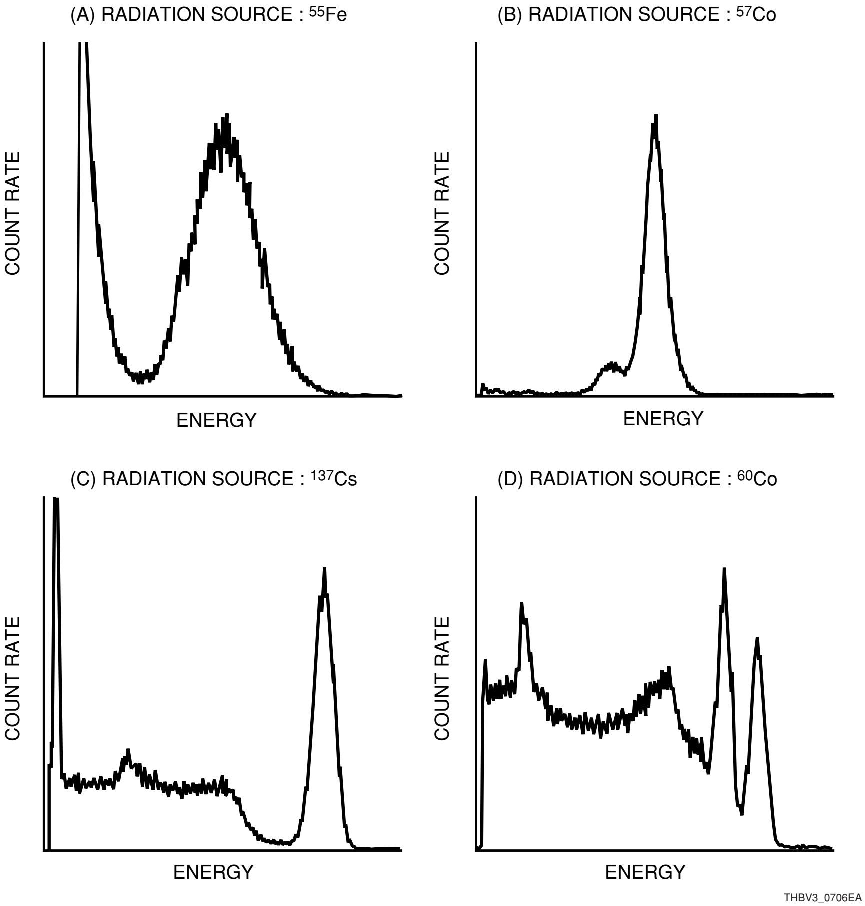

Figure 7-6: Typical pulse height distributions

The following factors affect the energy resolution.

(1) Energy conversion efficiency of the scintillator

(2) Intrinsic energy resolution of the scintillator

(3) Light collection efficiency of the photomultiplier tube photocathode

(4) Quantum efficiency (η) of the photomultiplier tube photocathode

(5) Collection efficiency (α) at first dynode

(6) Fluctuations in the multiplier section of photomultiplier tube

Generally, energy resolution is given by

$$R^2(E) = R_S{}^2(E) + Rp^2(E) \quad \text{(Eq. 7-2)}$$

where

$$R_P{}^2(E) = \frac{5.56}{N\eta\alpha}\left(\frac{\delta}{\delta-1}\right) \quad \text{(Eq. 7-3)}$$

in which N is the average number of photons incident on the photocathode per unit disintegration, η is the quantum efficiency, α is the collection efficiency and σ is the secondary emission yield at each dynode (assumed to be constant here).

In the above equations, Rs(E) is the energy resolution of the scintillator and Rp(E) is that of the photomultiplier tube, both of which depend on the energy (E) of the incident gamma ray. $Rp^2(E)$ is inversely proportional to E.

When a 2-inch diameter by 2-inch length NaI(Tl) scintillator and a 2-inch diameter photomultiplier tube (Hamamatsu R6231) are used, R, Rs and Rp will be approximately as follows:

With E =122 keV (^{57}Co), R = 8.5 %, Rs = 6 %, Rp = 6%

With E = 662 keV (^{137}Cs), R = 6.5 %, Rs = 5.5 %, Rp = 3.4 %

To obtain higher energy resolution, the photomultiplier tubes must have high quantum efficiency and collection efficiency. Along with using a scintillator with high conversion efficiency and good inherent energy resolution, good optical coupling between the scintillator and the photomultiplier tube should be provided to reduce optical loss. For this purpose, as mentioned previously it is helpful to couple the scintillator and the photomultiplier tube using silicone oil having an index of refraction close to that of the faceplate of the photomultiplier tube.

When the scintillator is sufficiently thick, the intensity distribution of light entering the photomultiplier tube is always constant over the photocathode regardless of the radiation input position, so the photomultiplier tube uniformity has little effect on the energy resolution. However, if the scintillator is thin, the distribution of light flash from the scintillator varies with the radiation input position. This may affect the energy resolution depending on the photomultiplier tube uniformity. To avoid this problem, a light-guide is sometimes placed between the scintillator and the photomultiplier tube so that the light flash from the scintillator is diffused and allowed to enter uniformly over the photocathode. But this technique is not necessary when using a photomultiplier tube with normal uniformity.

γ-ray source	Energy (keV)	NaI(Tl) + PMT	BGO + PMT
^{55}Fe	5.9	40 to 50%	—
^{241}Am	59.5	12 to 15%	70 to 150%
^{57}Co	122	8.5 to 10%	35 to 50%
^{22}Na	511	7.5 to 9.0%	13 to 25%
^{137}Cs	662	6.5 to 8.5%	11 to 20%
^{60}Co	1,170	5 to 6.5%	8.5 to 11%
	1,330	4.5 to 5.5%	8.0 to 9.5%

Table 7-2: Energy resolution for typical gamma-rays, obtained with NaI(Tl) or BGO scintillator

Energy resolution is one of the most important characteristics in radiation measurement such as gamma cameras and spectrometers. Photomultiplier tubes used in these applications are usually tested for energy resolution. Table 7-2 summarizes energy resolution for typical gamma rays measured with a NaI(Tl)/photomultiplier tube or a BGO/photomultiplier tube combination device. As shown in the table, each data has a certain width in energy resolution. This is due to the non-uniformity of the physical size of the scintillator or photomultiplier tube and also the performance variations between individual photomultiplier tubes. If necessary, it is possible to select only those photomultiplier tubes that meet specific specifications.

(2) Relative pulse height

In scintillation counting, when a photomultiplier tube is operated at a constant supply voltage and the amplification factor of the measuring circuit is fixed, the variation of the pulse height at a photoelectric peak is referred to as the relative pulse height (RPH) and is commonly stated in terms of the channel number. This relative pulse height indicates the variation of the pulse height obtained with a photomultiplier tube in scintillation counting. It usually shows a good correlation with measurement data taken by users (instrument manufacturers) and is therefore used to select the gain range of photomultiplier tubes. When used with a NaI(Tl) scintillator, the relative pulse height provides a close correlation with blue sensitivity because the emission spectrum of the NaI(Tl) resembles the spectral transmittance of the Corning filter CS No.5-58 which is used for the blue sensitivity measurement, so the relative pulse height has a strong correlation with the anode blue sensitivity index. (Refer to 4.1.5 in Chapter 4.)

(3) Linearity

Linearity of the output pulse height of a photomultiplier tube with respect to the amount of scintillation flash is another important parameter to discuss. Since linearity of general-purpose photomultiplier tubes has already been described earlier, this section explains how to measure linearity related to scintillation counting. Figure 7-7 shows a typical pulse height distribution for the ^{226}Ra taken with a NaI(Tl) and Figure 7-8 indicates the relationship between each peak channel and the gamma-ray energy. Because ^{226}Ra releases various kinds of radiation ranging in energy from 10.8 keV to 2.2 MeV, it is used for linearity measurements over a wide energy range.

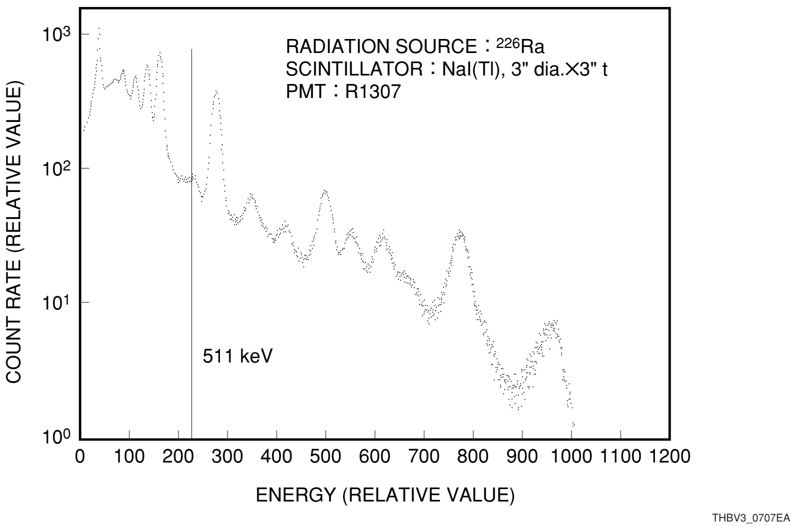

Figure 7-7: Pulse height distribution for ^{226}Ra taken with NaI(Tl)

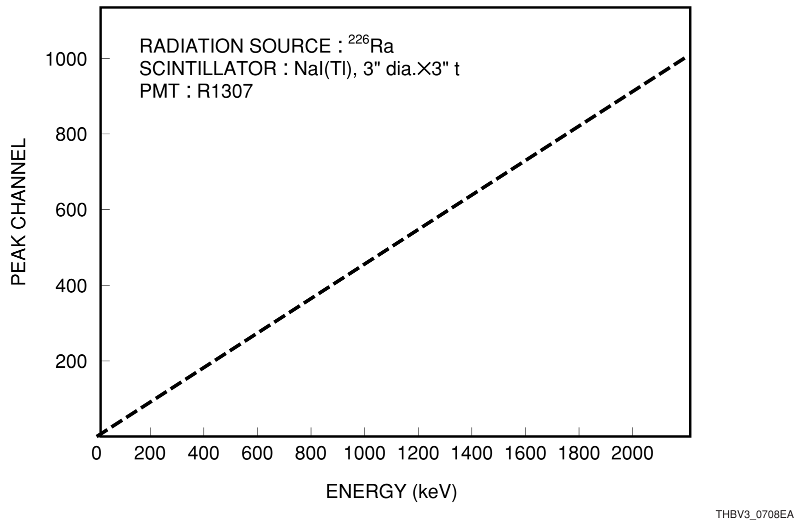

Figure 7-8: Relation between peak channel and gamma-ray energy

Amount of emission from a NaI(Tl) scintillator equals about 30 photons per 1 keV of gamma-ray energy. Accordingly, some 20,000 photons (662 keV × 30) are generated with ^{137}Cs and some 40,000 photons (1330 keV × 30) are generated with ^{60}Co. When ^{60}Co is used for linearity measurements under the conditions that the photomultiplier tube gain is at 10^6 and the decay constant (τ s) of the NaI(Tl) scintillator is 230 nanoseconds, the photomultiplier tube output current (Ip) is given by

$$Ip = \frac{N \times \eta \times \alpha \times \mu \times e}{\tau s} \quad \text{(Eq. 7-4)}$$

$$= \frac{4 \times 10^4 \times 0.25 \times 0.9 \times 10^6 \times 1.6 \times 10^{-19}}{230 \times 10^{-9}}$$

$$= 6.3 \times 10^{-3} (A)$$

N : amount of light flash per event produced from scintillator
η : quantum efficiency of photocathode (assumed to be 25 %)
α : collection efficiency of photomultiplier tube (assumed to be 90 %)
μ : gain of photomultiplier tube
e : electron charge
τs : decay time of NaI(Tl)

Thus in this measurement the photomultiplier tube must have a pulse linearity over 6.3 milliamperes. In particular, care should be taken with respect to the linearity range when measuring radiation at higher energy levels as the photomultiplier tube detects a large amount of light flash.

(4) Uniformity

The uniformity of a photomultiplier tube affects the performance of systems utilizing scintillation counting, especially in such equipment as Anger cameras used to detect the incident position of radiation. Uniformity of a photomultiplier tube is commonly defined as the variation in the output current with respect to the photocathode position on which a light spot is scanned.

However, another evaluation method like that illustrated in Figure 7-9 provides more useful data which allows users to predict the direct effects of uniformity on the equipment.

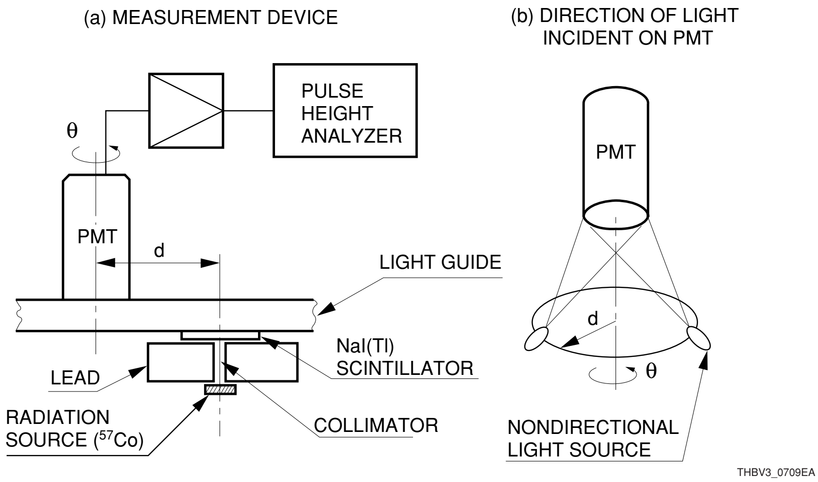

Figure 7-9: Measurement method for azimuth uniformity

In Figure 7-9, the photomultiplier tube is set at a distance (d) from a light source. The output variations of the photomultiplier tube are measured while the light source is rotated around the tube (by changing angle θ). The same procedure is repeated at different values of d. Then plotting the positions (d, θ) of the light source providing equal output gives a graph similar to a contour map (Figure 7-10). Uniformity data evaluated by this method is called the azimuth uniformity.

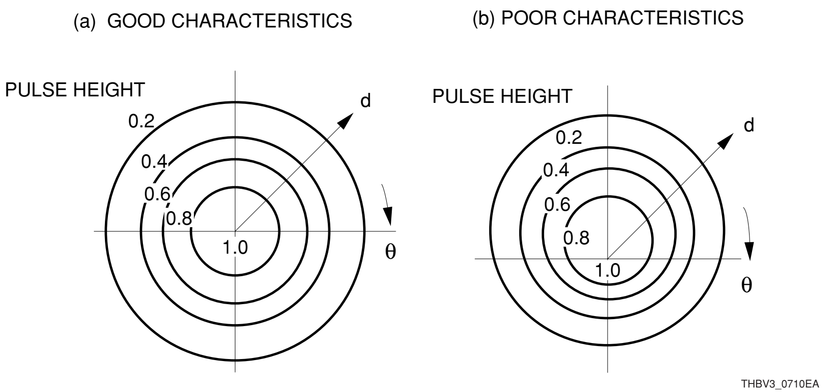

Figure 7-10: Examples of azimuth uniformity data

(5) Stability

There are two types of stability tests used in scintillation counting: long term stability and short term stability. Both stability tests employ a ^{137}Cs radiation source and a NaI(Tl) scintillator. The variation in the photopeak obtained from a photomultiplier tube is measured with a pulse height analyzer (PHA). These stability tests differ slightly from those applied to the general-purpose photomultiplier tubes which were discussed in the previous section.

a) Long term stability

The long term stability is also referred to as the photopeak drift. In this stability test, the photomultiplier tube is allowed to warm up for one hour with the photopeak count rate maintained at 1 ks^{-1}. After this, the variation rate of the photopeak pulse height (channel number) is measured for a period of 16 hours.

The same measurement setup shown in Figure 7-2 is used and the variation occurring in the peak channel is recorded as the time elapses. This variation (D_{LTD}) is calculated by Eq. 7-5 and typical variation data is shown in Figure 7-11 below.

$$D_{LTS} = \frac{\sum_{n=1}^{n} |Pi-\overline{P}|}{n} \cdot \frac{100}{\overline{P}} \quad \text{(Eq. 7-5)}$$

where

$\overline{P}$: mean value of photopeak pulse height (channel)
Pi: peak pulse height at the i-th reading
n : total number of readings for 16 hours

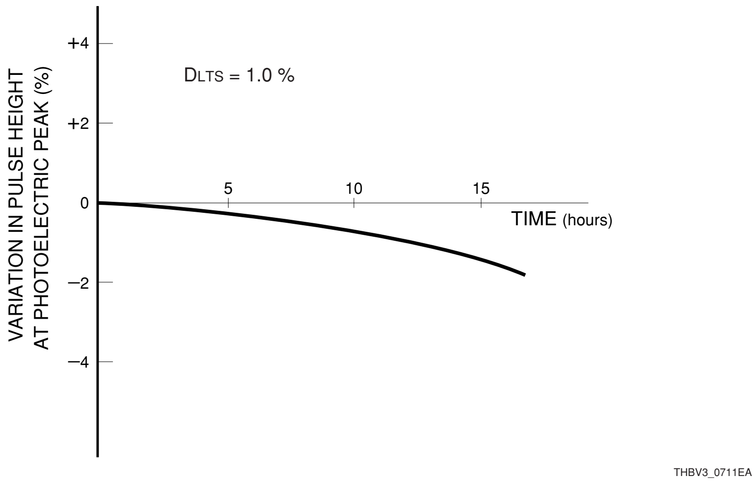

Figure 7-11: Typical long-term stability of photomultiplier tube

There are a few photomultiplier tube types that exhibit somewhat of a tendency to increase variation in photopeak pulse height during the period of 16 hours. However, most photomultiplier tubes tend to show decreasing values, with a variation rate within plus or minus several percent. This tendency is analogous to the drift characteristic explained earlier, but this test method is more practical for scintillation applications. Numerically, as shown in Eq. 7-5, the long term stability is defined as the mean deviation of the peak pulse height (or mean gain deviation) with respect to the mean pulse height. It usually has a value of 1 or 2 percent. A major cause of this output variation is that the secondary electron multiplication factor of the dynodes (particularly at the latter stages) changes over time.

b) Short term stability

The short term stability is also referred to as the count rate stability or count rate dependence. To evaluate this stability, the variation in the photopeak pulse height is measured by changing the photopeak count rate from 10 ks^{-1} to 1 ks^{-1}. If the photopeak pulse height at a count rate of 10 ks^{-1} is given by A and that at 1 ks^{-1} by B, the variation (D_{STS}) is given by the following equation. This value is expected to be about ±1 percent.

$$D_{STS} = (1-\frac{B}{A}) \times 100\ (\%) \quad \text{(Eq. 7-6)}$$

It is thought that this output instability is caused mainly by a change of the electron trajectories occurring in the electron multiplier section of a photomultiplier tube. This instability is also caused by a change in the voltage applied to the latter-stage dynodes, which may occur when operated at a high count rate and the output current increases to near the voltage-divider current. (Refer to 5.2.3 in Chapter 5.) In this case, photomultiplier tubes whose gain is less dependent on voltage (the slope of gain-voltage curve is not sharp) are less affected by the dynode voltage change. Short term stability is also closely related to the hysteresis effect in photomultiplier tubes. (Refer to 4.3.5 in Chapter 4.)

(6) Noise

In scintillation counting, a signal pulse is usually produced by multiple photoelectrons simultaneously emitted from the photocathode, which create a higher pulse height than most dark current pulses do. Using a discriminator effectively eliminates most dark current pulses with lower amplitudes. Accordingly, only noise pulses with higher amplitudes will be a problem in scintillation counting. To remove this type of noise pulse, the coincident counting technique is commonly used.

Noise pulses with higher amplitudes may be caused by radiation released from natural radioactive elements contained in a reinforced concrete building or in the atmosphere. These noise pulses may be a significant problem, particularly in low-level-radiation measurements. Concrete used to construct a building usually contains Rn, Th and ^{40}Fe, and steel contains U, Th and ^{60}Co. Radioactive floating dust and Rn or Th gases may be present in the atmosphere, and a scintillator may also contain minute amounts of ^{40}K and ^{208}Tl. Furthermore, borosilicate glass used to fabricate the faceplate of photomultiplier tubes contains potassium of which ^{40}K comprises 0.118 percent. The ^{40}K releases gamma rays of 1.46 MeV which can also be a cause of high-amplitude noise pulses.

Figure 7-12 shows background noise data measured with a Hamamatsu R877 photomultiplier tube (5-inch diameter, borosilicate glass, bialkali photocathode) coupled to a NaI(Tl) scintillator (5-inch diameter × 2-inch length). (1) in Figure 7-12 is measured without taking any countermeasures, while (2) is measured by shielding the tube with two lead blocks of 100 and 50 millimeter thickness, each being placed respectively in the lower section and upper section. (3) is data taken with an R877-01 that employs a so-called K-free glass containing a very minute amount of potassium for its faceplate and side bulb envelope.

Since these measurements were made using the setup in which the peak of ^{137}Cs (662 keV) becomes 300 channels, the energy range measured covers from about several keV to 2.2 MeV. In this energy range, the background noise, which is as high as 470 s^{-1} during normal measurement, can be drastically reduced to 26 s^{-1} (about 1/20) by shielding the tube with lead blocks. This means that most background noise originate from environmental radiation. In addition, use of the R877-01 with K-free glass (refer to 4.1.2 Chapter 4) further reduces the total noise counts down to about 16 s^{-1}. Particularly, in the energy range from 1.2 to 1.6 MeV where noise count mainly results from the ^{40}K (1.46 MeV), the noise count of 3.3 s^{-1} measured with the R877 (normal borosilicate glass) is reduced to 0.9 s^{-1} (below 1/3) with the R877-01 (K-free glass).

Recently in high energy physics experiments, there is a demand for photomultiplier tubes using materials that contain extremely low levels of radioactive impurities. Such experiments are often performed deep underground where natural radioactive impurities are eliminated and therefore impose heavy demands on the photomultiplier tubes to be used there. Glass materials used for these photomultiplier tubes must be investigated to make sure the content of radioactive impurities, not only ^{40}K but also uranium and thorium series, is sufficiently low.

The external parts of a photomultiplier tube and the scintillator are usually maintained at ground potential. Therefore, a cathode ground scheme with the high voltage applied to the anode is often used in scintillation counting. (Refer to 5.1.2 in Chapter 5.)

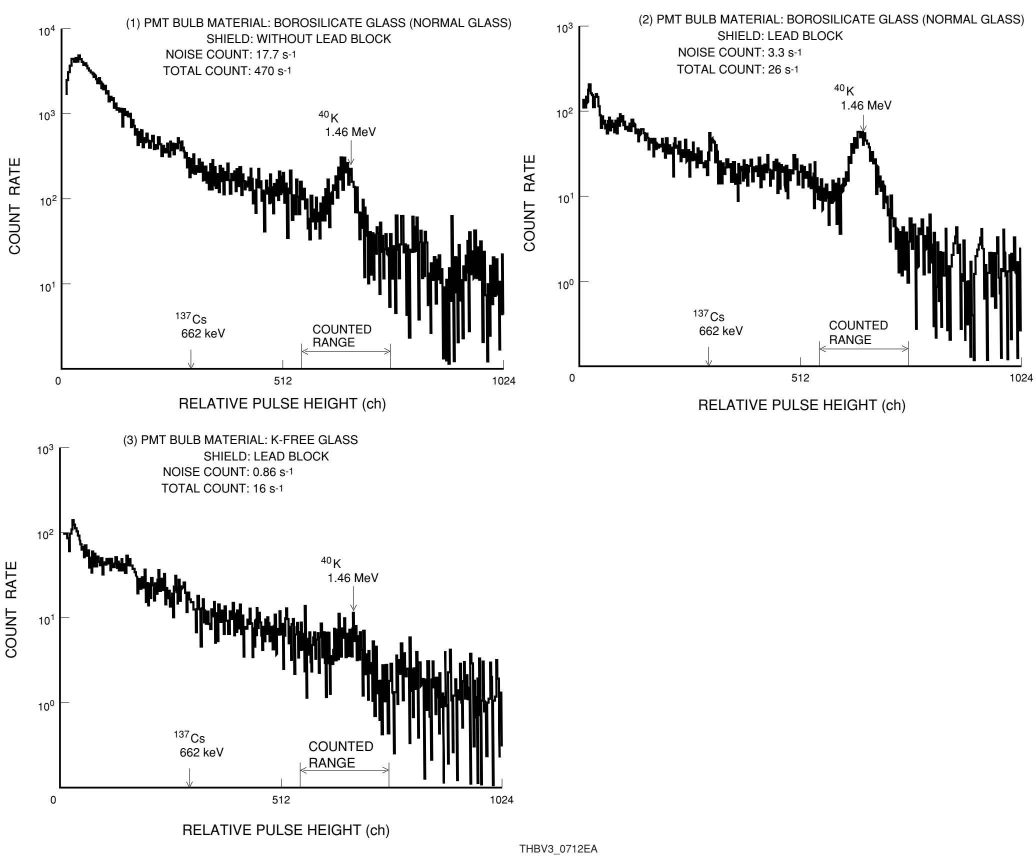

Figure 7-12: Background noise of 5-inch photomultiplier tube + NaI(Tl)

(7) Plateau characteristic

As stated, there are two measurement methods in scintillation counting. One method called the spectrum method that uses a pulse height analyzer has already been explained. This section will describe the other method called the counting method that does not use a pulse height analyzer. In the counting method, plateau characteristics are very important. Plateau characteristics are measured by setting a discrimination level and counting all pulses with amplitudes greater than that level. This operation is done while changing the supply voltage for the photomultiplier tube. Figure 7-13 (a) shows a block diagram for plateau characteristic measurement. Figures 7-13 (b) and (c) show typical plateau characteristics and pulse height distribution when a NaI(Tl) scintillator and ^{55}Fe radiation source are used.

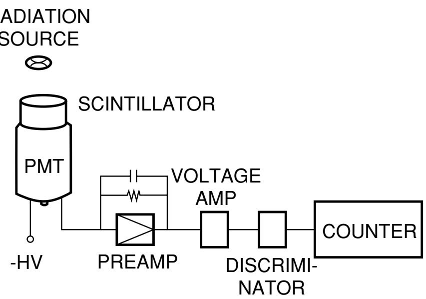

Figure 7-13 (a): Block diagram for plateau characteristic measurement

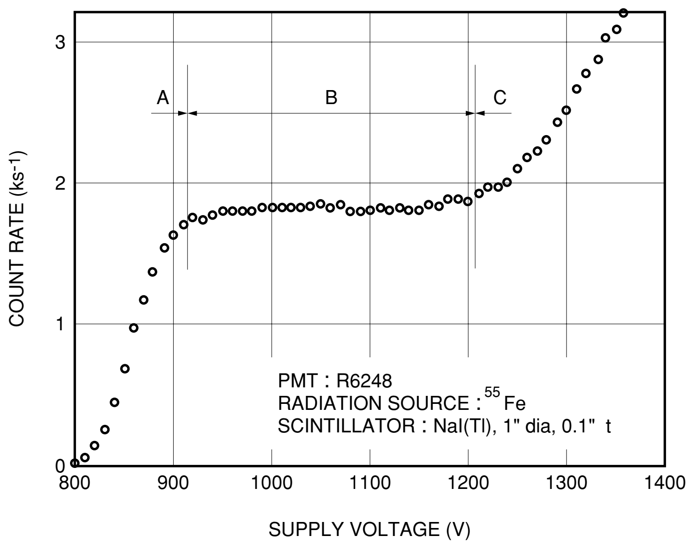

Figure 7-13 (b): Example of plateau characteristics

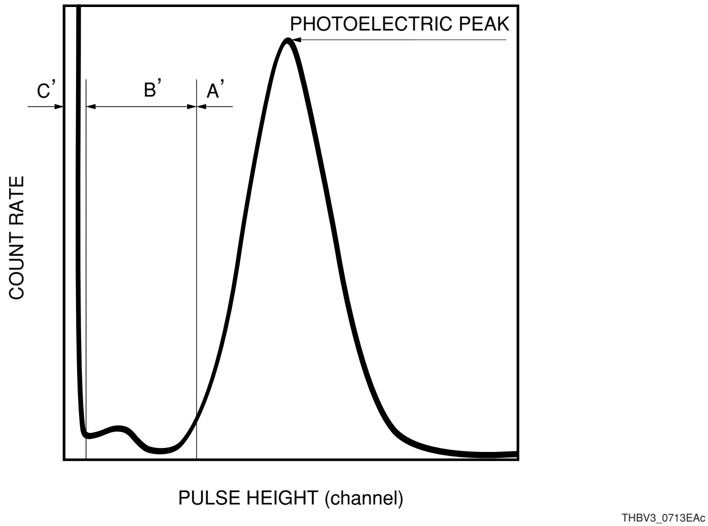

Figure 7-13 (c): Pulse height (^{55}Fe and NaI(Tl) combination)

The photomultiplier tube supply voltage is increased while the discrimination level is kept constant, the output pulses are counted in order from the photopeak region to the valley and the dark current regions. Plotting the count rate versus the photomultiplier tube supply voltage gives a curve like that shown in Figure 7-13 (b). This data can be divided into three regions (A, B and C). Region B is referred to as the plateau, and the supply voltage should be set within this region. The count rate will not vary even if the supply voltage is changed within this region, showing a constant photopeak count rate. The wider the plateau region, the less the count rate will be affected by fluctuations in the dark current. This plateau region corresponds to the valley of a pulse height distribution, that is, region B' in Figure 7-13 (c). Photomultiplier tubes with better energy resolution and lower dark current pulses provide a wider region B'.

As an application example, plateau characteristics are widely employed to evaluate photomultiplier tubes designed for use in oil well logging (refer to 14.5 in Chapter 14). In this application, geological strata type and density are measured by detecting and analyzing the number of scattered radiations or natural radiations from strata. Photomultiplier tubes used for oil well logging (sometimes called "high-temperature photomultiplier tubes") are usually tested in combination with a ^{137}Cs radiation source and a NaI(Tl) scintillator. Typical plateau characteristics obtained by this test are shown in Figure 7-14.

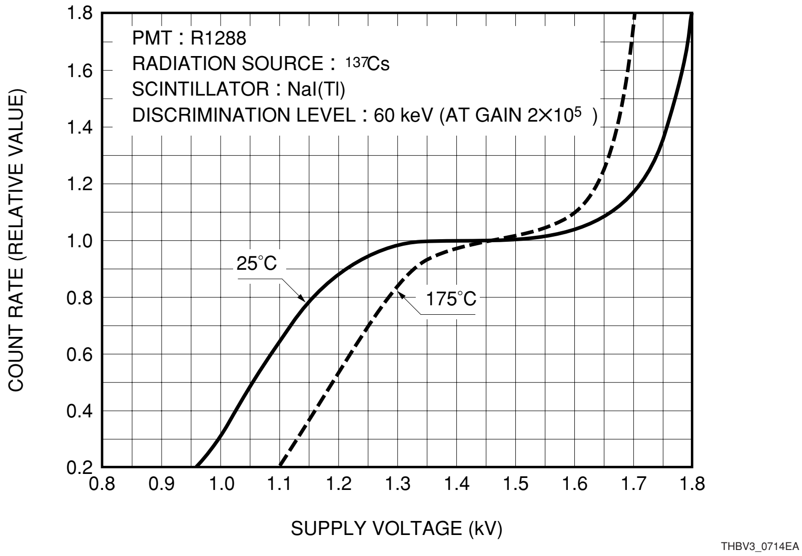

Figure 7-14: Typical plateau characteristics of a high-temperature photomultiplier tube

In the measurement shown in Figure 7-14, a photomultiplier tube designed for high temperature operation is used. The plateau characteristic taken at 175°C is shown along with that obtained at 25°C. Because the gain of the photomultiplier tube decreases as the temperature increases, the supply voltage at which the signal appears (corresponding to region A in Figure 7-13 (b)) shifts to the higher voltage side. The dark current on the other hand increases with temperature, so its count rate sharply increases (corresponding to region C in Figure 7-13 (b)) at a low supply voltage. Consequently, the plateau width (supply voltage range) measured at a higher temperature (175°C) becomes narrower than that obtained at room temperatures (25°C).

References in Chapter 7

1) Glenn. F. Knoll: "RADIATION DETECTION and MEASUREMENT (Third Edition)" John Wiley & Sons, Inc. (1999).
2) Nicholas Tsoulfanidis: "Measurement and Detection of Radiation", Hemispherev Publication Corporation (1983).
3) William J. Price: "Nuclear Radiation Detection", McGraw-Hill Book Company Inc. (1964).
4) Emil Kowalski: "Nuclear Electronics", Springer-Verlag Berlin (1970).
5) H. Kume, T. Watanabe, M. Iida, T. Matsushita and S. Suzuki: IEEE Trans. Nucl. Sci, NS-33[1], 364 (1986).
6) R.L. Heath, R. Hofstadter and E. B. Hughes: Nucl. Inst. and Meth, 162, 431 (1979).

MEMO